Electronic Supplementary Material (ESI) for Lab on a Chip.

Supplementary Information

Rapid formation of size-controllable multicellular spheroids *via* 3D acoustic tweezers

Kejie Chen, Mengxi Wu, Feng Guo, Peng Li, Chung-Yu Chan, Zhangming Mao, Sixing Li, Liqiang Ren, Rui Zhang, and Tony Jun Huang[*]

Department of Engineering Science and Mechanics, The Pennsylvania State University, University Park, PA 16802, USA

[*] *Address correspondence to junhuang@psu.edu*

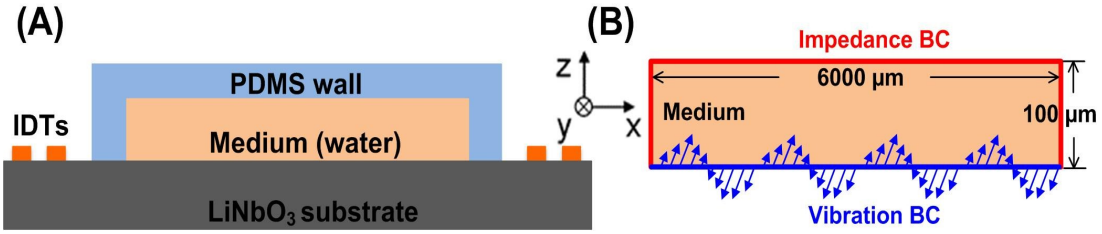

Figure S1 The computational domain and boundary conditions (BC). (A) Schematic of the acoustic tweezers based patterning device: a PDMS chamber, medium inside the chamber, and a $LiNbO_3$ piezoelectric substrate. (B) The computational domain is the medium inside the microfluidic chamber. The chamber's wall is modeled as an acoustically lossy wall BC, whereas the $LiNbO_3$ substrate is modeled as a vibrating BC with both longitudinal and transverse displacements.

Table S1 Parameters for numerical solution

PDMS chamber		
Length (l_1): 6000 μm	Width (l_2): 6000 μm	Height (l_3): 100 μm
Speed of sound	c_w	1076.5 m/s
Density	ρ_w	920 Kg/m^3
Water		
Density	ρ_0	997 Kg/m^3
Speed of sound	c_0	1497 m/s
Shear viscosity	μ	0.890 mPa · s
Bulk viscosity	μ_b	2.47 mPa · s
$LiNbO_3$ substrate		
Density	ρ_s	4640 Kg/m^3
Speed of sound	c_s	3994 m/s
Acoustic frequency	f	13.35 MHz
Cell		
Density	ρ_p	1075 Kg/m^3
Speed of sound	c_p	1600 m/s

Patterning polystyrene beads using acoustic tweezers

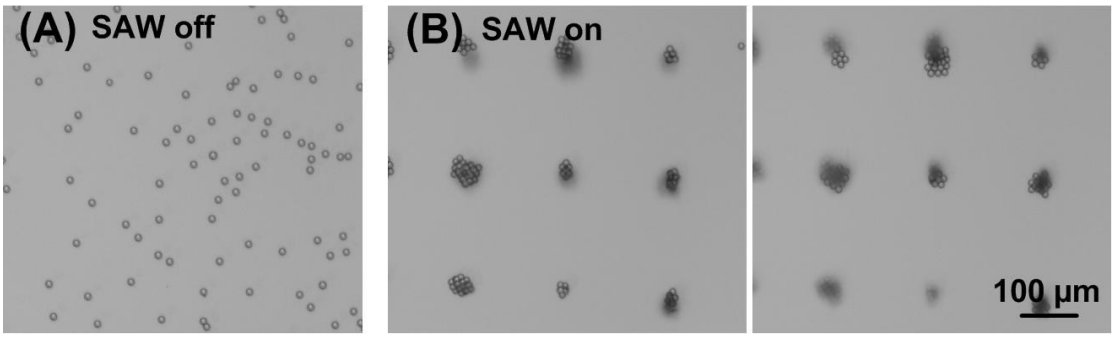

Fig. S2. Patterning of 10 μm polystyrene beads using acoustic tweezers. (A) When the SAW was off, the beads inside the PDMS chamber dispersed uniformly. (B) When the SAW was on, beads aggregated in the areas subjected to the lowest acoustic radiation force. The two images in (B) are different focuses at the same position: the beads are distributed in 3D environment.

The influence of acoustic power on cell trapping results

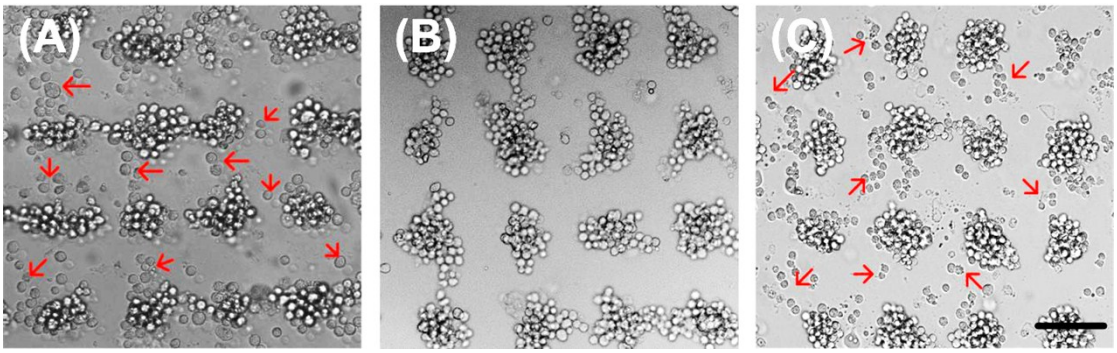

Fig. S3. Cells were trapped under different acoustic powers. (A) Under 25 dBm, part of cells remained quiescence and cannot be moved to the trapping nodes due to insufficient forces. (B) Under 30 dBm, cells can be efficiently moved to the trapping nodes and form into spheroids. (C) Under 35 dBm, cells near the substrate cannot be efficiently levitated up and moved to the trapping nodes because of the large acoustic radiation force. Red arrows mark the unpattern cells. Scale bar is 100 μm.

The influence of chamber height on trapping properties

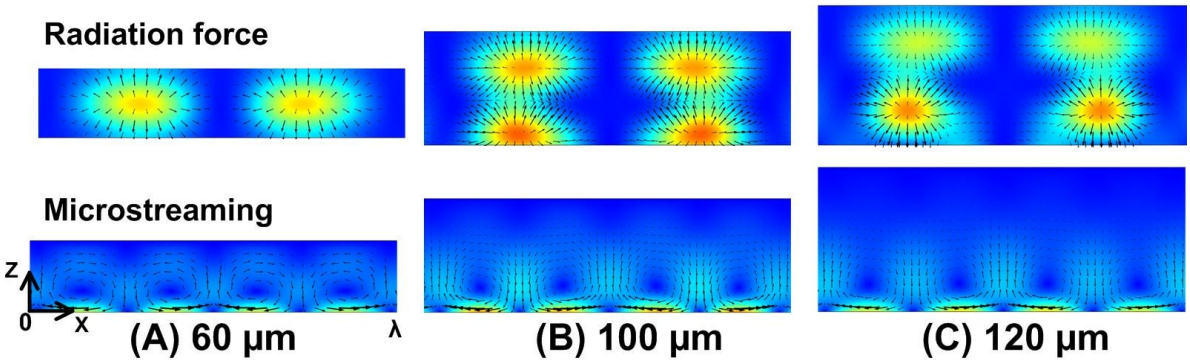

Fig. S4. Simulation of the distribution of acoustic radiation force and acoustic streaming force around pressure nodes with different chamber height. (A) When the chamber height is 60 μm, cells cannot be vertically "piled up" due to the limited space. (B) 100 ± 5 μm is the best height for spheroid formation. (C) When the chamber height is 120 μm, the acoustic field in the vertical plane becomes more complex and cells are separated into two vertical layers.

Patterning of HEK 293 spheroids arrays and cell viability test

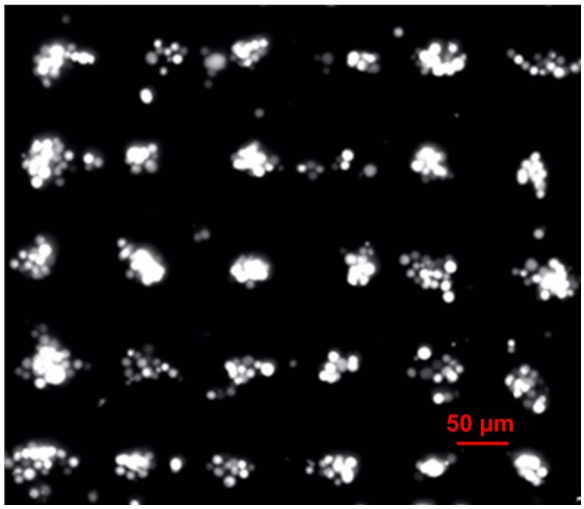

Movie S1. Patterning of HEK 293 spheroids arrays using acoustic tweezers. HEK 293 cells were labeled with Calcein AM to show the cell viability during acoustic tweezers-based patterning. Cells aggregated into spheroidal structure when subjected with the lowest acoustic potential. The movie is in real-time.

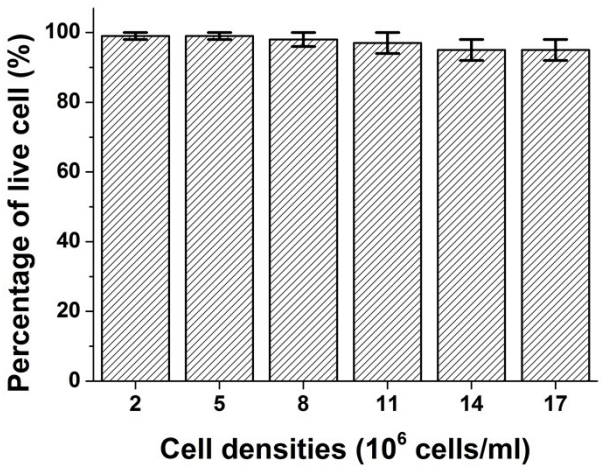

Fig. S5. The survival rate of HEK293 cells in spheroidal aggregates after turning on SAW for 20 min.

HepG2 cell aggregates under confocal microscope

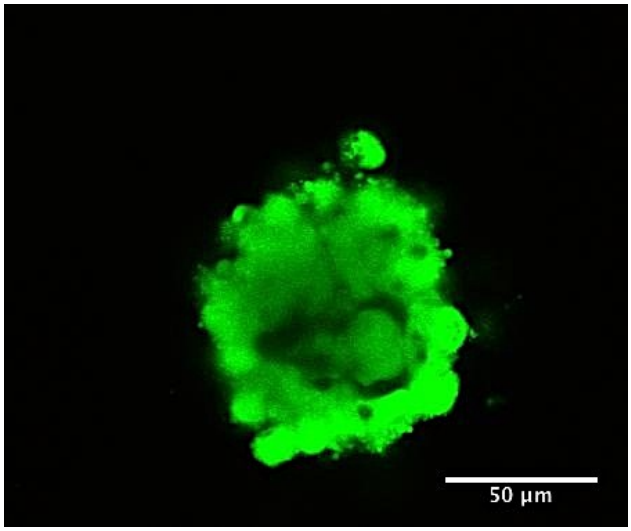

Movie S2. Different layers in vertical direction of HepG2 spheroids under confocal fluorescent microscopy. The HepG2 spheroid was fabricated by the acoustic tweezers method and cultured for 4 days. HepG2 cells were labeled with Calcein AM to show the cell viability.

Magnified images of HepG2 spheroids after anti-cancer drug testing

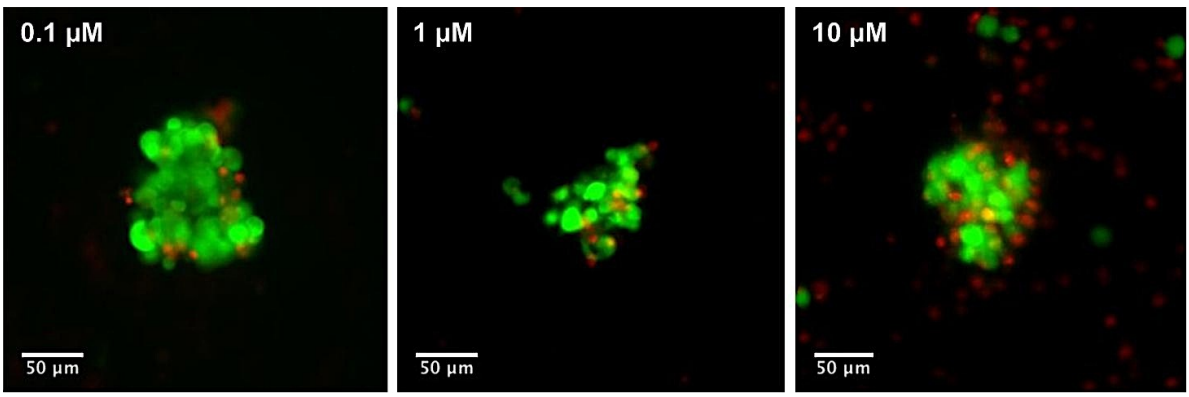

Fig. S6. Magnified images of HepG2 spheroids after anti-cancer drug testing.

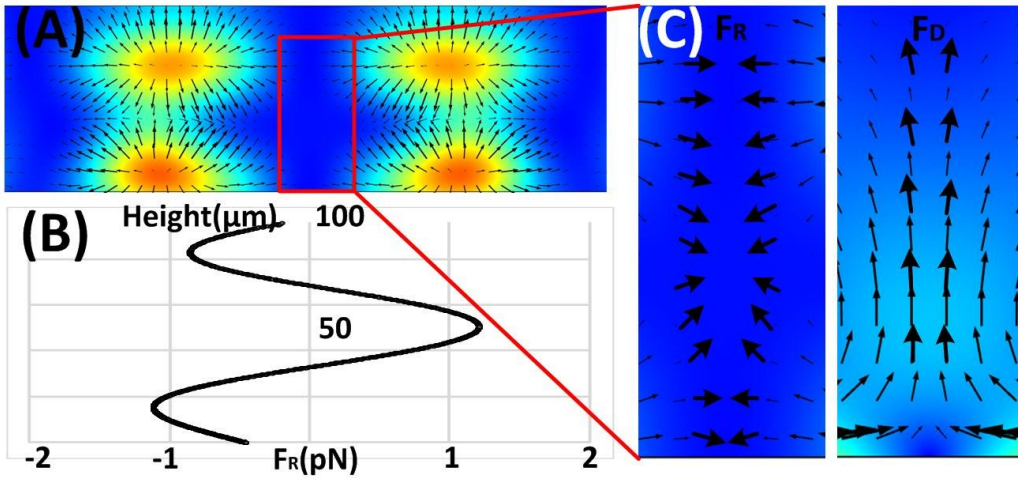

Fig. S7. (A) (C) The simulation results of acoustic radiation force and drag force from microstreaming above a pressure node. (B) The calculated magnitude distribution of acoustic radiation force in vertical direction above a pressure node. The minus magnitude of acoustic radiation force represents that the direction of the force is pointing down.